


2020

Asymptotic behavior of the average local ionization energy in finite basis sets

Amer M. El-Samman

Viktor N. Staroverov

Follow this and additional works at: <https://ir.lib.uwo.ca/chempub>

 Part of the [Chemistry Commons](#)

RESEARCH ARTICLE | OCTOBER 05 2020

Asymptotic behavior of the average local ionization energy in finite basis sets

Amer M. El-Samman ; Viktor N. Staroverov  



J. Chem. Phys. 153, 134109 (2020)

<https://doi.org/10.1063/5.0023459>

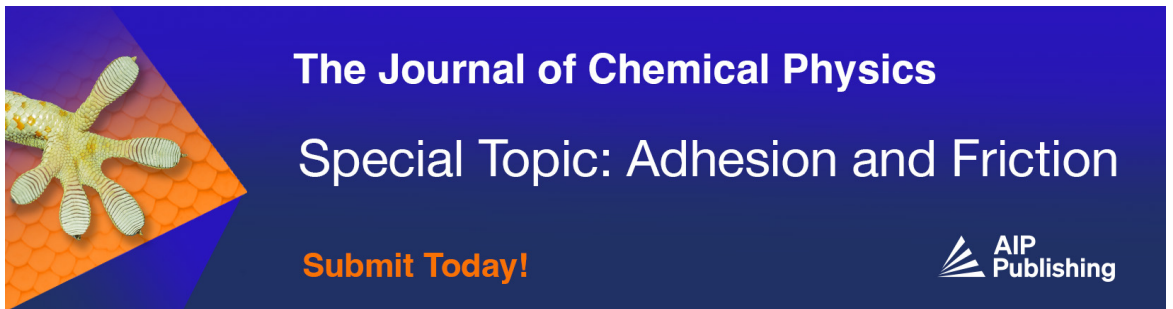


View
Online



Export
Citation

CrossMark



The Journal of Chemical Physics
Special Topic: Adhesion and Friction
Submit Today!
AIP Publishing

Asymptotic behavior of the average local ionization energy in finite basis sets

Cite as: J. Chem. Phys. 153, 134109 (2020); doi: 10.1063/5.0023459

Submitted: 29 July 2020 • Accepted: 16 September 2020 •

Published Online: 5 October 2020



View Online



Export Citation



CrossMark

Amer M. El-Samman  and Viktor N. Staroverov^{a)} 

AFFILIATIONS

Department of Chemistry, The University of Western Ontario, London, Ontario N6A 5B7, Canada

^{a)} Author to whom correspondence should be addressed: vstarove@uwo.ca

ABSTRACT

The average local ionization energy (ALIE) has important applications in several areas of electronic structure theory. Theoretically, the ALIE should asymptotically approach the first vertical ionization energy (IE) of the system, as implied by the rate of exponential decay of the electron density; for one-determinantal wavefunctions, this IE is the negative of the highest-occupied orbital energy. In practice, finite-basis-set representations of the ALIE exhibit seemingly irregular and sometimes dramatic deviations from the expected asymptotic behavior. We analyze the long-range behavior of the ALIE in finite basis sets and explain the puzzling observations. The findings have implications for practical calculations of the ALIE, the construction of Kohn–Sham potentials from wavefunctions and electron densities, and basis-set development.

Published under license by AIP Publishing. <https://doi.org/10.1063/5.0023459>

I. INTRODUCTION

The quantity known as average local ionization energy (ALIE) naturally arises in diverse contexts of electronic structure theory.^{1–11} For a single closed-shell N -electron Slater determinant of the spin-restricted Hartree–Fock (HF) method and the Kohn–Sham (KS) density-functional scheme, the ALIE is defined by

$$\bar{I}(\mathbf{r}) \equiv -\bar{\epsilon}(\mathbf{r}) = -\frac{2}{\rho(\mathbf{r})} \sum_{i=1}^{N/2} \epsilon_i |\phi_i(\mathbf{r})|^2, \quad (1)$$

where $\phi_i(\mathbf{r})$ are the occupied canonical orbitals, ϵ_i are their eigenvalues, and

$$\rho(\mathbf{r}) = 2 \sum_{i=1}^{N/2} |\phi_i(\mathbf{r})|^2 \quad (2)$$

is the total electron density. The name ALIE owes to the fact that $\bar{I}(\mathbf{r})$ is a position-dependent average of electron removal energies according to Koopmans' theorem.¹ The quantity $\bar{\epsilon}(\mathbf{r}) = -\bar{I}(\mathbf{r})$ is called the average local electron energy (ALEE) because it may be written^{11,12} in an orbital-invariant form as a sum of the local kinetic energy per electron and the effective potential in which each electron moves.

The ALIE and ALEE can also be defined for correlated wavefunctions in terms of the eigenfunctions and eigenvalues of the generalized Fock operator^{12–14} or, equivalently, in terms of the Dyson orbitals and associated electron removal energies.^{15,16} Because $\bar{I}(\mathbf{r})$ and $\bar{\epsilon}(\mathbf{r})$ are trivially related by a sign change, from now on we will refer to the ALEE only.

This work is concerned with one particular property of the ALEE—its asymptotic limit. For any ALEE given by Eq. (1), this limit is determined by the long-range behavior of the occupied molecular orbitals (MOs). The rate of exponential decay of KS orbitals is governed by their respective eigenvalues,^{17,18} whereas the asymptotically leading terms of HF orbitals generally share the same exponent and differ only by pre-exponential factors.^{19–21} In either case, the highest-occupied molecular orbital (HOMO) has the slowest overall rate of asymptotic decay. From this it follows that, for one-determinantal wavefunctions in a complete basis set and outside of the nodal surfaces of the HOMO,

$$\lim_{r \rightarrow \infty} \bar{\epsilon}(\mathbf{r}) = \epsilon_{\text{HOMO}}, \quad (3)$$

where ϵ_{HOMO} is the HOMO energy. The analog of Eq. (3) for an exact correlated wavefunction is¹²

$$\lim_{r \rightarrow \infty} \bar{\epsilon}(\mathbf{r}) = -I, \quad (4)$$

where I is the first vertical ionization energy of the system. Note that ϵ_{HOMO} and I are implied by the rates of the asymptotic exponential decay of the HF^{19–21} and exact electron densities,^{22–25} respectively. The properties expressed by Eqs. (3) and (4) play a key role in ensuring that the exchange-correlation potentials constructed from electronic wavefunctions^{9,10,26–29} have the proper asymptotic behavior and correct step structure.^{30–32}

We will now show that, within finite basis sets, Eqs. (3) and (4) may be satisfied exactly, approximately, or not at all, depending on subtle features of the one-electron basis set used. Our analysis will expose fundamental limitations of representing the ALEE function in finite basis sets, reveal occasional qualitative differences between comparable Gaussian basis sets, and explain why generation of KS effective potentials from wavefunctions and densities is sometimes hampered by diffuse basis functions. The conclusions apply to both Gaussian-type orbitals (GTO) and Slater-type orbitals (STO).

All calculations reported in this work were carried out using a locally modified version of the GAUSSIAN program.³³ All basis sets except cc-pVXZ and aug-cc-pVXZ match their definitions in the Basis Set Exchange Database³⁴ and include pure d , f , and higher functions. The cc-pVXZ and aug-cc-pVXZ basis sets were used, as implemented in GAUSSIAN—with linear transformations to remove redundant primitives from the contractions³⁵ (see the supplementary material).

II. ASYMPTOTIC LIMIT OF THE ALEE FOR ONE-DETERMINANTAL WAVEFUNCTIONS

A. Observations

In theory, the asymptotic limit of the quantity $\tilde{\epsilon}(\mathbf{r})$ defined by Eq. (1) is determined by the long-range behavior of the slowest-decaying occupied MO. In a complete basis set, the slowest-decaying MO is the HOMO, hence Eq. (3). The situation is very different in a finite basis set, where each MO is a linear combination of the same M basis functions,

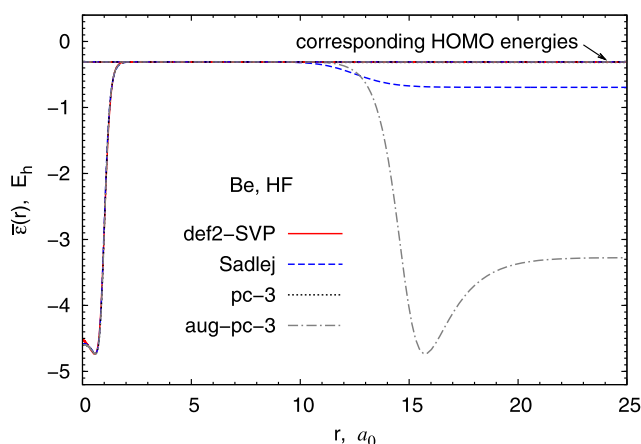


FIG. 1. HF ALEEs of the Be atom generated using various Gaussian basis sets. The presence of diffuse functions in Sadlej and aug-pc-3 causes large errors at $r > 9a_0$.

TABLE I. HOMO energies and asymptotic limits of the ALEE calculated from HF wavefunctions of the Be atom using various Gaussian basis sets.

Basis set	Size ^a	$\epsilon_{\text{HOMO}}, E_h$	a_{lim}, E_h^b
STO-3G	[2s]	−0.254 038	−0.256 733
6-31G	[3s]	−0.301 295	−0.301 524
6-31+G	[4s]	−0.307 177	−0.308 015
def2-SVP	[3s]	−0.305 431	−0.307 738
Sadlej	[5s]	−0.309 102	−0.693 831
cc-pVDZ	[3s]	−0.309 039	−0.309 224
cc-pVTZ	[4s]	−0.309 254	−0.309 413
cc-pVQZ	[5s]	−0.309 260	−0.309 339
cc-pV5Z	[6s]	−0.309 264	−0.309 278
aug-cc-pVDZ	[4s]	−0.309 381	−0.373 589
aug-cc-pVTZ	[5s]	−0.309 276	−0.696 376
aug-cc-pVQZ	[6s]	−0.309 271	−0.526 132
aug-cc-pV5Z	[7s]	−0.309 271	−0.365 717
pc-1	[3s]	−0.308 006	−0.308 101
pc-2	[4s]	−0.308 894	−0.308 956
pc-3	[6s]	−0.309 263	−0.316 984
pc-4	[8s]	−0.309 258	−0.321 237
aug-pc-1	[4s]	−0.308 518	−0.318 582
aug-pc-2	[5s]	−0.308 803	−0.311 076
aug-pc-3	[7s]	−0.309 262	−3.275 270
aug-pc-4	[9s]	−0.309 259	−1.066 429
UGBS	(25s)	−0.309 270	−0.309 277
Basis-set limit ^c		−0.309 270	−0.309 270

^aWithout the irrelevant p and d functions.

^bEvaluated using Eq. (9).

^cFrom Ref. 36.

$$\phi_i(\mathbf{r}) = \sum_{\mu=1}^M c_{\mu i} f_{\mu}(\mathbf{r}). \quad (5)$$

Here, the long-range behavior of $\phi_i(\mathbf{r})$ is determined by the slowest-decaying (most diffuse) functions $f_{\mu}(\mathbf{r})$ appearing with nonzero expansion coefficients. Typically, the most diffuse functions of a basis set contribute not only to the HOMO but also to the lower-lying MOs. It is intuitively clear that, when this happens, the asymptotic limit of $\tilde{\epsilon}(\mathbf{r})$ should be below ϵ_{HOMO} . Figure 1 and Table I show that the actual deviations can range from negligible to enormous (several hartrees) even for a small atom. To understand these results quantitatively, we will need to analyze in detail how the most diffuse basis functions determine the asymptotic limit of the ALEE.

B. Slowest-decaying functions of a basis set

Let us substitute Eq. (5) into Eq. (1) and, assuming that the basis functions are real, write the result as

$$\tilde{\epsilon}(\mathbf{r}) = \frac{\sum_{\mu=1}^M \sum_{\nu=1}^M E_{\mu\nu} f_{\mu}(\mathbf{r}) f_{\nu}(\mathbf{r})}{\sum_{\mu=1}^M \sum_{\nu=1}^M D_{\mu\nu} f_{\mu}(\mathbf{r}) f_{\nu}(\mathbf{r})}, \quad (6)$$

where

$$E_{\mu\nu} = 2 \sum_{i=1}^{N/2} \epsilon_i c_{\mu i} c_{\nu i} \quad (7)$$

are elements of the energy-weighted density matrix and

$$D_{\mu\nu} = 2 \sum_{i=1}^{N/2} c_{\mu i} c_{\nu i} \quad (8)$$

are elements of the density matrix. Both of these matrices are symmetric.

When evaluating the asymptotic limit of the right-hand side of Eq. (6), only the products of the slowest-decaying basis functions need to be considered. The rate of the asymptotic decay of a primitive basis function is determined by its exponent, α , and angular quantum number, l . For functions of the same l , the slowest-decaying function is the one with the smallest α . For functions with the same α , the slowest-decaying function is the one with the greatest l . Thus, if the smallest exponent for a given basis set is α_0 , the slowest-decaying functions are those functions with α_0 that have the greatest l . The rate of decay of a contracted basis function is that of the slowest-decaying primitive appearing in the contraction.

For further analysis, it will be convenient to distinguish whether the slowest-decaying basis functions are centered at one point or at different points.

C. Slowest-decaying basis functions with a common center

If the slowest-decaying basis functions with an angular quantum number l share a common center, then the total number of such functions is $2l + 1$. We assume that at least one of them contributes to the ALEE (otherwise the entire set may be ignored). The analysis of this situation applies to both GTOs or STOs.

Case $l = 0$: The slowest-decaying basis function is a unique s orbital, which we denote by $f_1(\mathbf{r})$. From Eq. (6), we get

$$a_{\text{lim}} \equiv \lim_{r \rightarrow \infty} \tilde{\epsilon}(\mathbf{r}) = \frac{E_{11}}{D_{11}} = \frac{\sum_{i=1}^{N/2} \epsilon_i |c_{1i}|^2}{\sum_{i=1}^{N/2} |c_{1i}|^2}, \quad (9)$$

where c_{1i} is the expansion coefficient of $f_1(\mathbf{r})$ in $\phi_i(\mathbf{r})$. This limit is bounded, $\epsilon_1 \leq a_{\text{lim}} \leq \epsilon_{\text{HOMO}}$, and is the same in every direction. Examples of such situations include a single Be atom described with cc-pVXZ basis sets, the CH₂O molecule described with the def2-SVPD basis set (the s function with α_0 is that of the C atom), and many other systems. The HF ALEE plots of Be shown in Fig. 1 are in perfect agreement with the values of a_{lim} computed by Eq. (9).

Case $l = 1$: The slowest-decaying basis functions are a single set of three p orbitals, $f_1 = p_x$, $f_2 = p_y$, and $f_3 = p_z$. If these functions are centered at the origin and oriented along the coordinate axes, then only f_1 contributes to the ALEE in the x direction, only f_2 contributes in the y direction, and only f_3 contributes in the z direction. For each of these particular directions, Eq. (6) gives

$$a_{\text{lim}}^x = \lim_{x \rightarrow \pm\infty} \tilde{\epsilon}(x, y, z) = \frac{E_{11}}{D_{11}}, \quad (10)$$

$$a_{\text{lim}}^y = \lim_{y \rightarrow \pm\infty} \tilde{\epsilon}(x, y, z) = \frac{E_{22}}{D_{22}}, \quad (11)$$

$$a_{\text{lim}}^z = \lim_{z \rightarrow \pm\infty} \tilde{\epsilon}(x, y, z) = \frac{E_{33}}{D_{33}}. \quad (12)$$

For an arbitrary direction \mathbf{u} defined by the angles β_1 , β_2 , and β_3 between \mathbf{u} and the x , y , and z axes, respectively, we obtain

$$a_{\text{lim}}(\mathbf{u}) = \frac{\sum_{\mu=1}^3 \sum_{\nu=1}^3 E_{\mu\nu} \cos \beta_\mu \cos \beta_\nu}{\sum_{\mu=1}^3 \sum_{\nu=1}^3 D_{\mu\nu} \cos \beta_\mu \cos \beta_\nu}, \quad (13)$$

where $\cos \beta_\mu$ are the direction cosines. If the system has cylindrical symmetry with respect to the z axis (e.g., CO), then the limit $a_{\text{lim}}^x = a_{\text{lim}}^y = a_{\text{lim}}^{xy}$ are the same in every direction from the origin within the $z = 0$ plane, but distinct from a_{lim}^z . If the system has tetrahedral or higher symmetry (e.g., CH₄ and Ne), then a_{lim} is again isotropic.

Case $l > 1$: One can extend the above analysis to this case or use the following trick: Orient the system with respect to the coordinate axes in such a way that the direction of interest (\mathbf{u}) coincides with the z axis and consider the most diffuse basis function that does not vanish in the z direction (d_{z^2} , f_{z^3} , and so on), call it $f_1(\mathbf{r})$. For this setup, $a_{\text{lim}}(\mathbf{u}) = a_{\text{lim}}^z = G_{11}/D_{11}$. By rotating the system and transforming or recomputing the coefficients G_{11} and D_{11} , one can determine a_{lim} for any \mathbf{u} .

There are three possible outcomes of evaluating a_{lim} for finite-basis-set HF and KS wavefunctions.

Outcome 1: $a_{\text{lim}} = \epsilon_{\text{HOMO}}$ exactly. This happens when the slowest-decaying functions of the basis set contribute to the HOMO but not to any lower-lying MOs. A prime example is the Ne atom described with the def2-TZVP basis set (Fig. 2). The HOMO level of this system consists of three degenerate atomic $2p$ orbitals. Since the most diffuse functions of the def2-TZVP basis set are of p type ($\alpha_0 \approx 0.266$), they contribute exclusively to the HOMOs. As a result, the asymptotic limit of the ALEE is exactly equal to ϵ_{HOMO} in all directions.

Another example is the HF/6-311+G ALEE of Ne (Fig. 3). Here the smallest exponent ($\alpha_0 = 0.13$) is shared by s - and p -type functions. The p functions have a pre-exponential factor and decay more slowly, so $a_{\text{lim}} = \epsilon_{\text{HOMO}}$ again. However, the presence of an s function with the same α_0 slows down the asymptotic decay of $\tilde{\epsilon}(\mathbf{r})$ (compare

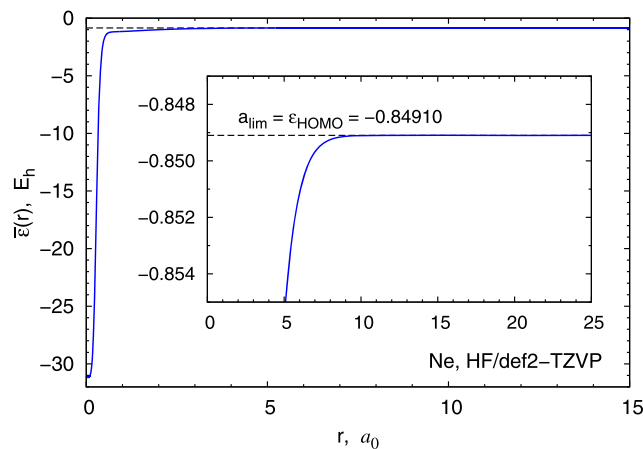


FIG. 2. HF/def2-TZVP ALEE for the Ne atom. The basis functions with the smallest exponent are of p type. The asymptotic limit is approached fast.

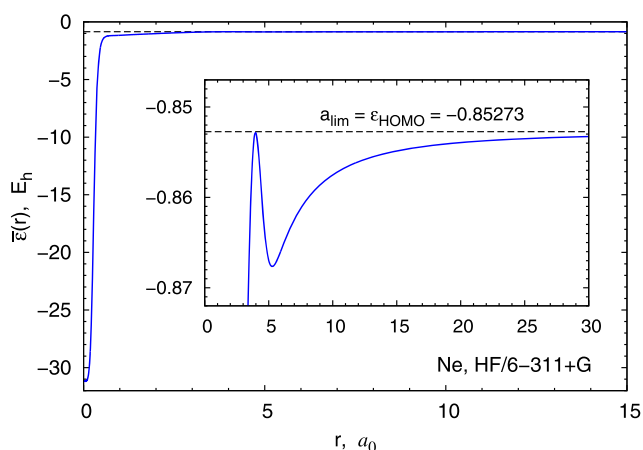


FIG. 3. HF/6-311+G ALEE for the Ne atom. The basis functions with the smallest exponent are of s and p types. The asymptotic limit is approached slowly.

Figs. 3 and 2). The inset of Fig. 3 reveals another interesting feature of this ALEE: a local maximum at $r \approx 4a_0$, where $\bar{\epsilon}(\mathbf{r})$ is equal to ϵ_{HOMO} almost exactly. This happens on the nodal sphere of the $2s$ orbital, where only the p functions contribute.

Outcome 2: $a_{\text{lim}} \approx \epsilon_{\text{HOMO}}$. This occurs when the slowest-decaying basis function makes the dominant, but not exclusive, contribution to the HOMO. Such behavior is exhibited by the HF/def2-SVP and HF/pc-3 ALEEs of the Be atom (Fig. 1). Figure 4 shows the former example in detail. The MO coefficients of the slowest-decaying s function of the def2-SVP basis set ($\alpha_0 \approx 0.0458$) are $c_{12} = 0.38024$ and $c_{11} = -0.00868$ in ϕ_2 and ϕ_1 , respectively. The ratio $|c_{12}|^2/|c_{11}|^2$ is large enough for $\bar{\epsilon}(\mathbf{r})$ to be close to ϵ_{HOMO} at large r . The point near $r = 4.4a_0$, where $\bar{\epsilon}(\mathbf{r}) = \epsilon_{\text{HOMO}}$ exactly, is the location of an artificial node of the $1s$ orbital arising in the HF/def2-SVP description of the Be atom. Artificial nodes are often

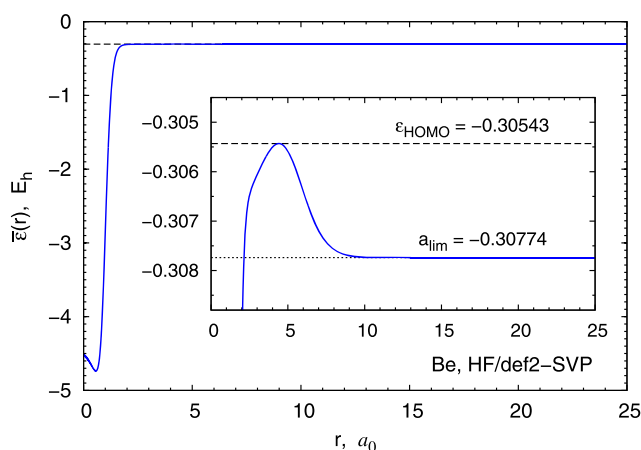


FIG. 4. HF/def2-SVP ALEE for the Be atom. The slowest-decaying s function contributes mostly to the HOMO. The asymptotic limit is only approximately equal to ϵ_{HOMO} .

found in the asymptotic tails of KS and HF orbitals, both in numerical and finite-basis-set solutions.^{37–39}

Outcome 3: $a_{\text{lim}} < \epsilon_{\text{HOMO}}$. This happens when the slowest-decaying basis function makes substantial contributions to at least one lower-lying MO. Such instances are common for basis sets containing diffuse functions. For example, the most diffuse s -type function of the Sadlej basis set for Be ($\alpha_0 \approx 0.0193$) has MO coefficients of 0.00575 and 0.00178 in ϕ_2 and ϕ_1 , respectively. As a result, $a_{\text{lim}} = -0.6938 E_h$ is significantly lower than $\epsilon_{\text{HOMO}} = -0.3091 E_h$ (Fig. 1). For the HF/aug-pc-3 ALEE of Be, the mismatch is even greater: $\epsilon_{\text{HOMO}} = -0.3093 E_h$, whereas $a_{\text{lim}} = -3.2753 E_h$. Our analysis makes it evident that the theoretical result $a_{\text{lim}} = \epsilon_{\text{HOMO}}$ cannot be reproduced exactly in a finite basis set whenever there is a lower-lying MO of the same symmetry as the HOMO, except when the canonical MOs themselves serve as basis functions.

The HF/def2-SVP ALEE of Ne (Fig. 5) illustrates another possible twist. Here the HOMO is of p type, but the slowest-decaying basis function is of s type, so the asymptotic behavior of $\bar{\epsilon}(\mathbf{r})$ is determined by the $1s$ and $2s$ orbitals and not at all by the HOMO. The closest approach of this ALEE to ϵ_{HOMO} occurs between 5 and 7 bohrs, where the HOMO contribution to the ALEE exceeds that of all other occupied orbitals.

Situations in which the most diffuse basis function is unique are not limited to atoms. Consider, for instance, the HF/DGDZVP ALEE of the CO molecule oriented along the z axis with the C atom at the origin (Fig. 6). The ground-state electron configuration of CO is $1\sigma^2 2\sigma^2 3\sigma^2 4\sigma^2 1\pi^4 5\sigma^2$. The slowest-decaying basis functions here are the three carbon-centered p -type primitive GTOs (p_x, p_y, p_z) with $\alpha_0 = 0.10972$. These functions contribute to MOs of different symmetries and energies: the p_z function to each of the σ -MOs including the HOMO, and the p_x and p_y functions to the π -MOs. By Eqs. (10)–(13), the ALEE limit along the z axis is $a_{\text{lim}}^z = -0.6154 E_h$; within the $z = 0$ plane, it is $a_{\text{lim}}^{xy} = -0.6418 E_h$, i.e., the energy of the π -MOs to which the p_x and p_z functions contribute exclusively. Neither of these two limits is even close to $\epsilon_{\text{HOMO}} = -0.5541 E_h$. To get a better agreement between a_{lim} and ϵ_{HOMO} for CO, it is necessary to use a

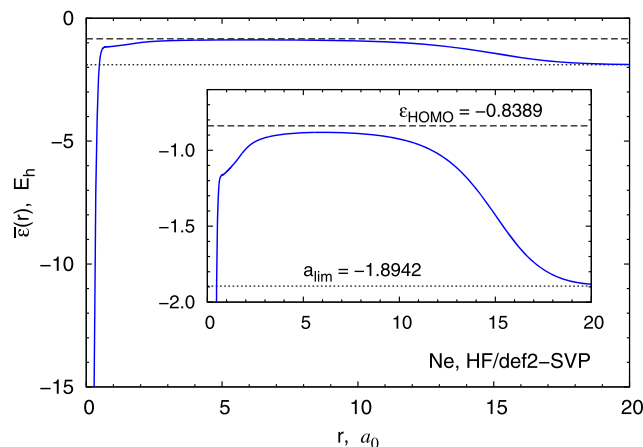


FIG. 5. HF/def2-SVP ALEE for the Ne atom. The slowest-decaying basis function is of s type. The asymptotic limit is substantially lower than ϵ_{HOMO} .

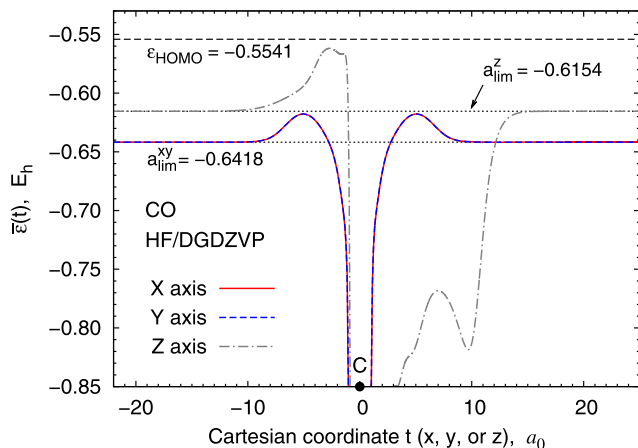


FIG. 6. HF/DGDZVP ALEE of the CO molecule ($R = 2.132a_0$) along the three coordinate axes. The molecule is oriented along the z axis with the C nucleus at the origin. The slowest-decaying basis functions are three p -type GTOs centered at the C nucleus.

different basis set in which the slowest-decaying basis function is of s type, e.g., def2-SVP ($a_{\text{lim}} = -0.5637 E_h$, $\epsilon_{\text{HOMO}} = -0.5510 E_h$).

D. Slowest-decaying basis functions with multiple centers

When the slowest-decaying functions of a basis set are centered at different points, the asymptotic limit of $\tilde{\epsilon}(\mathbf{r})$ always has angular dependence. Let us first analyze the case of two primitive s -type GTOs, $f_1(\mathbf{r})$ and $f_2(\mathbf{r})$, placed R bohrs apart and equivalent by symmetry (as in a homonuclear diatomic). Without loss of generality, we can assume that $f_1(\mathbf{r})$ and $f_2(\mathbf{r})$ are unnormalized and centered at the points $A = (0, 0, R/2)$ and $B = (0, 0, -R/2)$, respectively, that is,

$$f_1(\mathbf{r}) = e^{-\alpha_0[x^2+y^2+(z-R/2)^2]}, \quad (14)$$

$$f_2(\mathbf{r}) = e^{-\alpha_0[x^2+y^2+(z+R/2)^2]}. \quad (15)$$

Substituting these expressions into Eq. (6) and evaluating the $z \rightarrow \infty$ limit, we obtain

$$a_{\text{lim}}^z \equiv \lim_{z \rightarrow \pm\infty} \tilde{\epsilon}(x, y, z) = \frac{E_{11}}{D_{11}} = \frac{E_{22}}{D_{22}}, \quad (16)$$

where $E_{11} = E_{22}$ and $D_{11} = D_{22}$ by symmetry. Similarly, for directions perpendicular to the z axis at $z = t$, we find

$$\begin{aligned} a_{\text{lim}}^{xy}(t) &\equiv \lim_{x \rightarrow \pm\infty} \tilde{\epsilon}(x, y, t) = \lim_{y \rightarrow \pm\infty} \tilde{\epsilon}(x, y, t) \\ &= \frac{(1 + e^{4\alpha_0 R t})E_{11} + 2e^{2\alpha_0 R t}E_{12}}{(1 + e^{4\alpha_0 R t})D_{11} + 2e^{2\alpha_0 R t}D_{12}}, \end{aligned} \quad (17)$$

which is different from a_{lim}^z . In particular, for the xy planes passing through the nuclei,

$$a_{\text{lim}}^{xy}(\pm R/2) = \frac{(1 + e^{2\alpha_0 R^2})E_{11} + 2e^{\alpha_0 R^2}E_{12}}{(1 + e^{2\alpha_0 R^2})D_{11} + 2e^{\alpha_0 R^2}D_{12}}, \quad (18)$$

whereas for the xy plane at the midpoint,

$$a_{\text{lim}}^{xy}(0) = \frac{E_{11} + E_{12}}{D_{11} + D_{12}}. \quad (19)$$

The same relations apply to p -type GTOs centered at $(0, 0, \pm R/2)$: Eq. (16) to a pair of p_z functions and Eqs. (17)–(19) to pairs of p_x and p_y functions. Observe that Eq. (16) is for two GTOs but works as though there were only one function, as in Eq. (9).

It is important to remember that Eqs. (16)–(19) hold only for GTOs. For STOs, Eq. (6) gives different results,

$$a_{\text{lim}}^z = \frac{(1 + e^{2\alpha_0 R})E_{11} + 2e^{\alpha_0 R}E_{12}}{(1 + e^{2\alpha_0 R})D_{11} + 2e^{\alpha_0 R}D_{12}} \quad (\text{STO}) \quad (20)$$

and

$$a_{\text{lim}}^{xy}(t) = \frac{E_{11} + E_{12}}{D_{11} + D_{12}} \quad (\text{STO}) \quad (21)$$

both for s and p functions. The second of these limits no longer depends on t .

As a first test of Eqs. (16)–(19), consider the HF/pc-1 ALEE for the F_2 molecule oriented along the z axis (Fig. 7). The electron configuration is $KK(\sigma_g 2s)^2(\sigma_u^* 2s)^2(\pi_u 2p)^4(\sigma_g 2p)^2(\pi_g^* 2p)^4$. The slowest-decaying basis functions are primitive p -type Gaussians ($\alpha_0 = 0.31127$). The p_x and p_y functions make large contributions to the degenerate π_g^* HOMOs as well as to the lower-lying π_u MOs. This signals that a_{lim} values should be significantly below $\epsilon_{\text{HOMO}} = -0.6732 E_h$. For the xy plane passing through each nucleus, $a_{\text{lim}}^{xy} = -0.7484 E_h$, as predicted by Eq. (18) with $f_1 = p_x^A$ and $f_2 = p_x^B$. Along the z axis, $a_{\text{lim}}^z = -0.7747 E_h$, as predicted by Eq. (16) with $f_1 = p_z^A$ and $f_2 = p_z^B$.

Another example is the HF/6-311++G* ALEE of the H_2O molecule placed in the yz plane with z as the C_2 axis (Fig. 8). The ground-state electron configuration here is $1a_1^2 2a_1^2 1b_2^2 3a_1^2 1b_1^2$, and the slowest-decaying functions are two s -type primitives ($\alpha_0 = 0.036$).

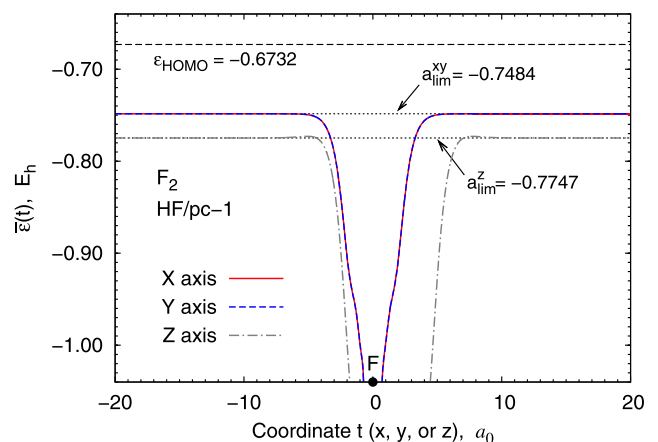


FIG. 7. HF/pc-1 ALEE of the F_2 molecule ($R = 2.670a_0$) along the three coordinate axes with one of the nuclei moved to the origin. The molecule is oriented along the z axis. The most diffuse basis functions are of p type.

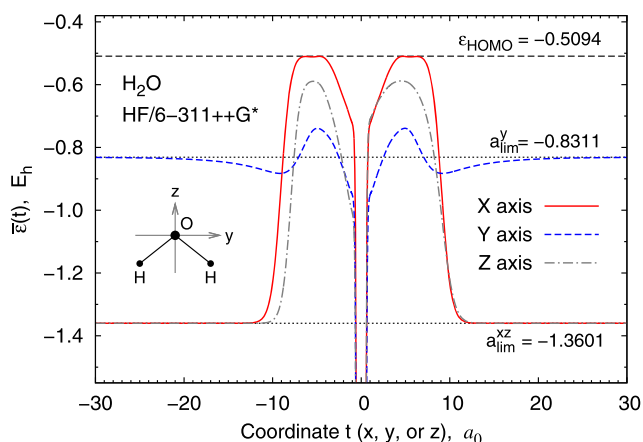


FIG. 8. HF/6-311++G* ALEE of the H₂O molecule ($R_{\text{OH}} = 1.810a_0$, $\theta_{\text{HOH}} = 104.5^\circ$) along the three coordinate axes. The molecule is oriented as shown. The most diffuse basis functions are two s -type GTOs of the H atoms.

centered at the H nuclei. These functions form symmetry-adapted linear combinations only of a_1 and b_2 symmetries and therefore cannot contribute to the b_1 HOMO (the nonbonding $2p_x$ atomic orbital of the O atom). As a result, all a_{lim} values here are much lower than $\epsilon_{\text{HOMO}} = -0.5094 E_h$. Specifically, $a_{\text{lim}}^y = -0.8311 E_h$, as predicted by Eq. (16) adapted to the current axis orientation, and $a_{\text{lim}}^x = a_{\text{lim}}^z = a_{\text{lim}}^{xz} = -1.3601 E_h$, as predicted by the similarly adapted equation (19).

If the slowest-decaying basis function for H₂O were an s -type GTO of the O nucleus (which is unusual for standard basis sets), the HF ALEE would have the same asymptotic limit in every direction but still would be substantially lower than ϵ_{HOMO} , because an s -type function of the O atom cannot contribute to the b_1 HOMO. If the slowest-decaying basis functions were a set of three p GTOs of the O atom (as in 6-311+G* and def2-SVPD), then a_{lim} would equal ϵ_{HOMO} exactly but only along the x axis; in other directions, it would be a weighted average of the energies of all MOs to which p -type basis functions of the O atom contribute. For the ALEE of H₂O to approach ϵ_{HOMO} everywhere except in the nodal plane of the HOMO, one would need a customized basis set in which the slowest-decaying function is a p_x GTO without the accompanying p_y and p_z orbitals.

III. ASYMPTOTIC LIMIT OF THE ALEE FOR CORRELATED WAVEFUNCTIONS

The one-determinantal ALEE of Eq. (1) can be generalized to spin-restricted correlated wavefunctions in several equivalent ways.^{12–14,16} The form best suited for computation is¹²

$$\tilde{\epsilon}(\mathbf{r}) = \frac{2}{\rho(\mathbf{r})} \sum_{j=1}^K \lambda_j |g_j(\mathbf{r})|^2, \quad (22)$$

where $g_j(\mathbf{r})$ are the eigenfunctions of the generalized Fock operator, λ_j are their eigenvalues, and $K \geq N/2$. For a closed-shell Slater determinant, $K = N/2$, $g_j(\mathbf{r}) = \phi_j(\mathbf{r})$, and $\lambda_j = \epsilon_j$, so Eq. (22) reduces to Eq. (1).¹² For a complete active space (CAS) self-consistent-field

(SCF) wavefunction, K is the total number of the core and active orbitals. For a full configuration interaction (FCI) wavefunction, $K = M$. Although the magnitudes of λ_j for post-HF wavefunctions are no longer associated with electron removal energies, the negative of the generalized ALEE can still be interpreted as an ALIE.¹⁶

Let us write the generalized ALEE in terms of a basis set of real functions $f_\mu(\mathbf{r})$ ($\mu = 1, 2, \dots, M$). Each eigenfunction $g_j(\mathbf{r})$ has the form

$$g_j(\mathbf{r}) = \sum_{\mu=1}^M b_{\mu j} f_\mu(\mathbf{r}), \quad (23)$$

where the coefficients $b_{\mu j}$ are determined by diagonalizing the generalized Fock matrix. The total electron density may be written as

$$\rho(\mathbf{r}) = 2 \sum_{j=1}^K n_j |\chi_j(\mathbf{r})|^2, \quad (24)$$

where $\chi_j(\mathbf{r})$ are the natural orbitals and n_j are their occupation numbers ($0 < n_j \leq 1$). Each natural orbital may be expanded in the same one-electron basis set,

$$\chi_j(\mathbf{r}) = \sum_{\mu=1}^M q_{\mu j} f_\mu(\mathbf{r}), \quad (25)$$

where the coefficients $q_{\mu j}$ are obtained by diagonalizing the one-electron reduced density matrix. Substituting Eqs. (23)–(25) into Eq. (22), we obtain

$$\tilde{\epsilon}(\mathbf{r}) = \frac{\sum_{\mu=1}^M \sum_{\nu=1}^M G_{\mu\nu} f_\mu(\mathbf{r}) f_\nu(\mathbf{r})}{\sum_{\mu=1}^M \sum_{\nu=1}^M P_{\mu\nu} f_\mu(\mathbf{r}) f_\nu(\mathbf{r})}, \quad (26)$$

where

$$G_{\mu\nu} = 2 \sum_{j=1}^K \lambda_j b_{\mu j} b_{\nu j} \quad (27)$$

and

$$P_{\mu\nu} = 2 \sum_{j=1}^K n_j q_{\mu j} q_{\nu j}. \quad (28)$$

The matrix \mathbf{G} is symmetric for variationally optimal wavefunctions such as CASSCF and FCI.^{40–43}

One can use Eq. (26) to find the asymptotic limits of a generalized finite-basis-set ALEE in the same manner as Eq. (6) was used for HF wavefunctions. In particular, if the slowest-decaying function, $f_1(\mathbf{r})$, has $l = 0$, then

$$a_{\text{lim}} = \frac{G_{11}}{P_{11}} = \frac{\sum_{j=1}^K \lambda_j |b_{1j}|^2}{\sum_{j=1}^K n_j |q_{1j}|^2}, \quad (29)$$

where b_{1j} and q_{1j} are the coefficients of $f_1(\mathbf{r})$ in Eqs. (23) and (25), respectively. The other recipes are the same as Eqs. (9)–(19) with $E_{\mu\nu}$ replaced by $G_{\mu\nu}$ and $D_{\mu\nu}$ by $P_{\mu\nu}$.

For HF wavefunctions, we compared a_{lim} to ϵ_{HOMO} , expecting agreement in the basis-set limit. It is not immediately clear what a_{lim} should be compared to for correlated wavefunctions. The analysis of the long-range behavior of electronic wavefunctions by

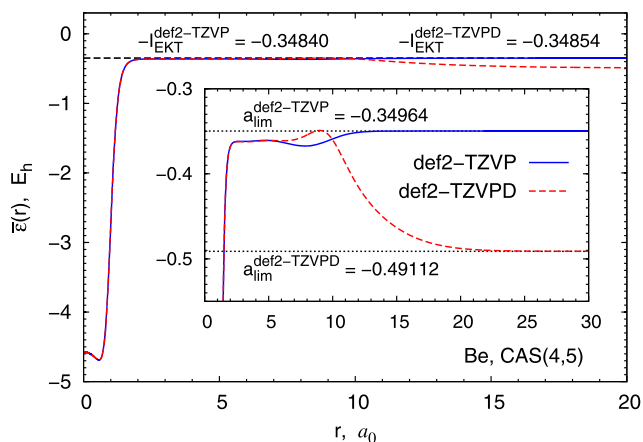


FIG. 9. Generalized ALEE for the Be atom computed from CAS(4,5) wavefunctions using two basis sets. The asymptotic limits were evaluated by Eq. (29).

Morrell *et al.*,²² Davidson,²³ and Katriel and Davidson²⁴ implies²⁷ that the asymptotic limit of $\bar{\epsilon}(\mathbf{r})$ is $-I$, i.e., the negative of the first ionization energy encoded in the rate of exponential decay of the natural orbitals, $\chi_k \propto \exp[-(2I)^{1/2}r]$ ($r \rightarrow \infty$). For HF wavefunctions in the basis-set limit, $I = -\epsilon_{\text{HOMO}}$,^{19–21} which leads to Eq. (3). This motivates us to estimate the I of Eq. (4) as the first ionization energy according to the extended Koopmans' theorem (EKT).^{22,44–46} The EKT is a well-defined computational prescription for variationally optimal wavefunctions such as HF and CASSCF.^{40–43}

As an example, consider the CAS(4,5) ALEE computed for the Be atom using two related basis sets: def2-TZVP and def2-TZVPD. The active space includes the 1s, 2s, 2p_x, 2p_y, and 2p_z orbitals, which means that the *p*-type functions of these basis sets contribute alongside *s* functions. The slowest-decaying functions of def2-TZVP and def2-TZVPD are, respectively, an *s*-type primitive ($\alpha_0 \approx 0.03265$) and a set of three *p*-type primitives ($\alpha_0 \approx 0.02773$). Using Eq. (29) for the former basis set and Eqs. (10)–(12) for the latter, we obtain $a_{\text{lim}}^{\text{def2-TZVP}} = -0.34964 E_h$ and $a_{\text{lim}}^{\text{def2-TZVPD}} = -0.49112 E_h$. These limits are in perfect agreement with the actual ALEE plots (Fig. 9). Although the def2-TZVP limit is very close to the corresponding $-I_{\text{EKT}}$ value, the def2-TZVPD limit is not. This suggests that the def2-TZVPD basis set is imbalanced for the purpose of representing the ALEE in low-density regions. The above analysis can be readily extended to basis sets in which the slowest-decaying functions are centered at multiple points.

IV. IMPLICATIONS

A. Calculation of ALEEs

The ALEE provides important information about chemical reactivity, electronegativity, local polarizability, hardness, and other molecular properties.^{1–3,47–50} Our findings suggest that the accuracy of $\bar{\epsilon}(\mathbf{r})$ at large r may be drastically affected by the type and location of the most diffuse basis functions. Therefore, it is essential to use a properly chosen or customized one-electron basis set when computing HF, KS, and post-HF ALEEs. Of course, by enforcing the

correct a_{lim} one does not necessarily attain the correct rate of asymptotic decay of $\rho(\mathbf{r})$. The latter property would require a considerably subtler customization of the basis set than discussed here.^{51–54}

B. Generation of exchange-correlation potentials from wavefunctions

In a series of papers,^{9,10,26–29} Staroverov and co-workers developed a method for constructing KS potentials from *ab initio* electronic wavefunctions within finite basis sets. This method involves solving the KS equations with the exchange-correlation potential given by

$$v_{\text{XC}}(\mathbf{r}) = v_{\text{XC}}^{\text{hole}}(\mathbf{r}) + v_{\text{resp}}(\mathbf{r}) + v_{c,\text{kin}}(\mathbf{r}), \quad (30)$$

where $v_{\text{XC}}^{\text{hole}}(\mathbf{r})$ is the Coulomb potential of the exchange-correlation hole charge, $v_{\text{resp}}(\mathbf{r})$ is the response term, and $v_{c,\text{kin}}(\mathbf{r})$ is the kinetic-correlation contribution. The response term is computed in our method as

$$v_{\text{resp}}(\mathbf{r}) = \bar{\epsilon}^{\text{KS}}(\mathbf{r}) - \bar{\epsilon}^{\text{WF}}(\mathbf{r}), \quad (31)$$

where $\bar{\epsilon}^{\text{WF}}(\mathbf{r})$ is the generalized ALEE of Eq. (22) and $\bar{\epsilon}^{\text{KS}}(\mathbf{r})$ is the KS ALEE of Eq. (1). The expressions for $v_{\text{XC}}^{\text{hole}}(\mathbf{r})$ and $v_{c,\text{kin}}(\mathbf{r})$ are irrelevant here (see Ref. 13 for details). The definitive version of this method is presented in Ref. 28.

Within Gaussian basis sets, the method of Ref. 28 produces exchange-correlation potentials of higher quality than any technique in which $v_{\text{XC}}(\mathbf{r})$ is fitted to $\rho(\mathbf{r})$. However, there is a limitation: when the basis set contains very diffuse functions, the potential of Eq. (30) may deviate from the correct $-1/r$ behavior at large r so much as to cause a failure of SCF convergence. This is a deterministic basis-set artifact that can be understood and remedied through the insights from Secs. II and III.

When the method of Ref. 28 is applied to HF wavefunctions, one needs to shift the KS spectrum obtained in each SCF cycle to satisfy the condition $\epsilon_{\text{HOMO}}^{\text{KS}} = \epsilon_{\text{HOMO}}^{\text{HF}}$. The aim of this shift is

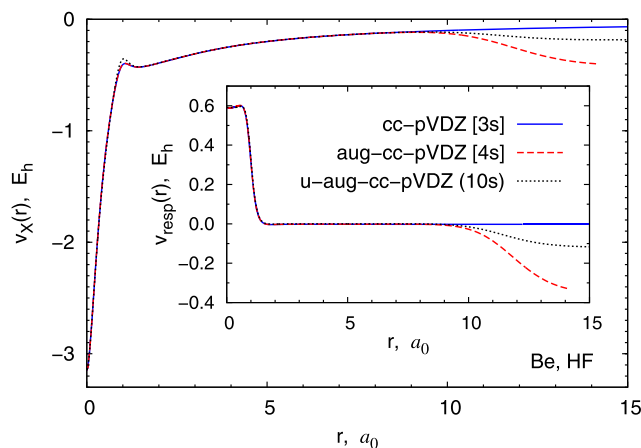


FIG. 10. Exact-exchange potentials and corresponding response terms calculated from HF wavefunctions of the Be atom using various Gaussian basis sets. To achieve SCF convergence for the aug-cc-pVDZ basis set, we ignored all grid points where $\rho(\mathbf{r})$ is below $2 \times 10^{-10} e/a_0^3$.

to force $\tilde{\epsilon}^{\text{KS}}(\mathbf{r})$ to have the same asymptotic limit as $\tilde{\epsilon}^{\text{HF}}(\mathbf{r})$. The equality of the two limits makes $v_{\text{resp}}(\mathbf{r})$ vanish asymptotically and enables $v_{\text{XC}}(\mathbf{r})$ to behave as $-1/r$ when $r \rightarrow \infty$. In a defective basis set, where $\tilde{\epsilon}^{\text{KS}}(\mathbf{r})$ and $\tilde{\epsilon}^{\text{HF}}(\mathbf{r})$ cannot simultaneously approach the HOMO energy, the shift fails to achieve the desired effect and the resulting $v_{\text{resp}}(\mathbf{r})$ tends to a nonzero constant. The error in $v_{\text{resp}}(\mathbf{r})$ causes a comparable error in $v_{\text{XC}}(\mathbf{r})$ (see Fig. 10) and, if large enough, impedes SCF convergence. A simple but effective fix in such cases is to set $v_{\text{resp}}(\mathbf{r}) = 0$ at grid points where $\rho(\mathbf{r})$ is very small (say, below $10^{-10} e/a_0^3$). Another remedy is to enable the HF and KS ALEEs to have the same asymptotic limit by tweaking the one-electron basis set. Similar considerations apply to potentials generated from post-HF wavefunctions and to other potential construction techniques that employ the quantity $\tilde{\epsilon}^{\text{KS}}(\mathbf{r})$.^{30,55}

Strictly speaking, these convergence problems are caused not by particular diffuse functions themselves but by their interplay with other basis functions. For instance, uncontracting the aug-cc-pVDZ basis set for Be does not affect any of the exponents but improves the ALEE and $v_{\text{XC}}(\mathbf{r})$ (Fig. 10).

V. CONCLUSIONS

We have shown that the asymptotic behavior of ALEEs calculated within finite basis sets may drastically deviate from theoretical predictions that assume a complete basis set. For a given system, basis set, and direction, the asymptotic limit a_{lim} of $\tilde{\epsilon}(\mathbf{r})$ may be determined analytically using Eq. (6) or Eq. (26). For systems where the slowest-decaying basis functions are centered at one or two points, the calculation of a_{lim} reduces to applying simple recipes such as Eqs. (9)–(12) and (16)–(19).

In theory, every one-determinantal ALEE should have $a_{\text{lim}} = \epsilon_{\text{HOMO}}$ outside of the nodal surfaces of the HOMO. A one-electron basis set can produce this result only if the most diffuse basis functions contribute exclusively to the HOMO. If this condition is not met (e.g., because there are other occupied MOs of the same symmetry as the HOMO), one can have $a_{\text{lim}} \approx \epsilon_{\text{HOMO}}$ at best. If the most diffuse functions make comparable contributions to the HOMO and to lower-energy MOs or do not contribute to the HOMO at all, then $a_{\text{lim}} \ll \epsilon_{\text{HOMO}}$.

For finite-basis-set ALEEs derived from correlated wavefunctions, the property expressed by Eq. (4) can hold only approximately in practice. This is because the strict equality $a_{\text{lim}} = -I$ requires the most diffuse functions of the basis set to contribute exclusively to the Dyson orbital associated with the lowest ionization energy, which does not happen for sets of GTOs or STOs.

We conclude with practical recommendations: (1) Suitability of a one-electron basis set for representing an ALEE can be assessed by comparing the magnitude of a_{lim} to the estimated ionization energy of the system (ϵ_{HOMO} for Slater determinants and I_{EKT} for correlated wavefunctions). (2) Methods for constructing KS exchange-correlation potentials from finite-basis-set electron densities and wavefunctions should employ basis sets in which the most diffuse functions have the type (*s*, *p*, *d*, and so on) and location suitable for representing ALEEs at large *r*. (3) Basis sets that do not produce accurate ALEE limits should be used with caution in calculations of long-range molecular properties.

SUPPLEMENTARY MATERIAL

See the [supplementary material](#) for complete specification of the transformed cc-pVXZ and aug-cc-pVXZ basis sets used to generate the data of Table I and Fig. 10.

ACKNOWLEDGMENTS

This work was supported by the Natural Sciences and Engineering Research Council (NSERC) of Canada through the Discovery Grants Program (Application No. RGPIN-2020-06420).

DATA AVAILABILITY

The data that support the findings of this study are available within the article and its [supplementary material](#).

REFERENCES

- 1 P. Sjöberg, J. S. Murray, T. Brinck, and P. Politzer, *Can. J. Chem.* **68**, 1440 (1990).
- 2 P. Politzer, F. Abu-Awwad, and J. S. Murray, *Int. J. Quantum Chem.* **69**, 607 (1998).
- 3 P. Politzer, J. S. Murray, and F. A. Bulat, *J. Mol. Model.* **16**, 1731 (2010).
- 4 Á. Nagy, R. G. Parr, and S. Liu, *Phys. Rev. A* **53**, 3117 (1996).
- 5 P. W. Ayers, R. G. Parr, and Á. Nagy, *Int. J. Quantum Chem.* **90**, 309 (2002).
- 6 A. Toro-Labbé, P. Jaque, J. S. Murray, and P. Politzer, *Chem. Phys. Lett.* **407**, 143 (2005).
- 7 O. Gritsenko, R. van Leeuwen, and E. J. Baerends, *J. Chem. Phys.* **101**, 8955 (1994).
- 8 A. A. Kananenka, S. V. Kohut, A. P. Gaiduk, I. G. Ryabinkin, and V. N. Staroverov, *J. Chem. Phys.* **139**, 074112 (2013).
- 9 I. G. Ryabinkin, A. A. Kananenka, and V. N. Staroverov, *Phys. Rev. Lett.* **111**, 013001 (2013).
- 10 S. V. Kohut, I. G. Ryabinkin, and V. N. Staroverov, *J. Chem. Phys.* **140**, 18A535 (2014).
- 11 F. A. Bulat, M. Levy, and P. Politzer, *J. Phys. Chem. A* **113**, 1384 (2009).
- 12 I. G. Ryabinkin and V. N. Staroverov, *J. Chem. Phys.* **141**, 084107 (2014).
- 13 R. Cuevas-Saavedra and V. N. Staroverov, *Mol. Phys.* **114**, 1050 (2016).
- 14 V. N. Staroverov, *Mol. Phys.* **117**, 1 (2019).
- 15 V. H. Smith and Y. Öhrn, in *Reduced Density Operators with Applications to Physical and Chemical Systems-II*, edited by R. M. Erdahl (Queen's University, Kingston, ON, 1974), pp. 193–200.
- 16 S. V. Kohut, R. Cuevas-Saavedra, and V. N. Staroverov, *J. Chem. Phys.* **145**, 074113 (2016).
- 17 C.-O. Almbladh and U. von Barth, *Phys. Rev. B* **31**, 3231 (1985).
- 18 P. Gori-Giorgi, T. Gál, and E. J. Baerends, *Mol. Phys.* **114**, 1086 (2016).
- 19 N. C. Handy, M. T. Marron, and H. J. Silverstone, *Phys. Rev.* **180**, 45 (1969).
- 20 G. S. Handler, D. W. Smith, and H. J. Silverstone, *J. Chem. Phys.* **73**, 3936 (1980).
- 21 T. Ishida and K. Ohno, *Theor. Chim. Acta* **81**, 355 (1992).
- 22 M. M. Morrell, R. G. Parr, and M. Levy, *J. Chem. Phys.* **62**, 549 (1975).
- 23 E. R. Davidson, *Reduced Density Matrices in Quantum Chemistry* (Academic, New York, 1976), pp. 55–56.
- 24 J. Katriel and E. R. Davidson, *Proc. Natl. Acad. Sci. U. S. A.* **77**, 4403 (1980).
- 25 M. Levy, J. P. Perdew, and V. Sahni, *Phys. Rev. A* **30**, 2745 (1984).
- 26 I. G. Ryabinkin, S. V. Kohut, and V. N. Staroverov, *Phys. Rev. Lett.* **115**, 083001 (2015).
- 27 R. Cuevas-Saavedra, P. W. Ayers, and V. N. Staroverov, *J. Chem. Phys.* **143**, 244116 (2015).
- 28 E. Ospadov, I. G. Ryabinkin, and V. N. Staroverov, *J. Chem. Phys.* **146**, 084103 (2017).

- ²⁹V. N. Staroverov and E. Ospadov, *Adv. Quantum Chem.* **79**, 201 (2019).
- ³⁰O. V. Gritsenko and E. J. Baerends, *Phys. Rev. A* **54**, 1957 (1996).
- ³¹S. V. Kohut, A. M. Polgar, and V. N. Staroverov, *Phys. Chem. Chem. Phys.* **18**, 20938 (2016).
- ³²I. G. Ryabinkin, E. Ospadov, and V. N. Staroverov, *J. Chem. Phys.* **147**, 164117 (2017).
- ³³M. J. Frisch, G. W. Trucks, H. B. Schlegel, G. E. Scuseria, M. A. Robb, J. R. Cheeseman, G. Scalmani, V. Barone, G. A. Petersson, H. Nakatsuji, X. Li, M. Caricato, A. V. Marenich, J. Bloino, B. G. Janesko, R. Gomperts, B. Men-
nucci, H. P. Hratchian, J. V. Ortiz, A. F. Izmaylov, J. L. Sonnenberg, D. Williams-
Young, F. Ding, F. Lipparini, F. Egidi, J. Goings, B. Peng, A. Petrone, T. Hen-
derson, D. Ranasinghe, V. G. Zakrzewski, J. Gao, N. Rega, G. Zheng, W. Liang,
M. Hada, M. Ehara, K. Toyota, R. Fukuda, J. Hasegawa, M. Ishida, T. Nakajima,
Y. Honda, O. Kitao, H. Nakai, T. Vreven, K. Throssell, J. A. Montgomery, Jr., J. E.
Peralta, F. Ogliaro, M. J. Bearpark, J. J. Heyd, E. N. Brothers, K. N. Kudin, V. N.
Staroverov, T. A. Keith, R. Kobayashi, J. Normand, K. Raghavachari, A. P. Rendell,
J. C. Burant, S. S. Iyengar, J. Tomasi, M. Cossi, J. M. Millam, M. Klene, C. Adamo,
R. Cammi, J. W. Ochterski, R. L. Martin, K. Morokuma, O. Farkas, J. B. Fores-
man, and D. J. Fox, GAUSSIAN Development Version, Revision I.13, Gaussian, Inc.,
Wallingford, CT, 2016.
- ³⁴B. P. Pritchard, D. Altarawy, B. Didier, T. D. Gibson, and T. L. Windus, *J. Chem.
Inf. Model.* **59**, 4814 (2019).
- ³⁵E. R. Davidson, *Chem. Phys. Lett.* **260**, 514 (1996).
- ³⁶T. Koga, *Theor. Chem. Acc.* **95**, 113 (1997).
- ³⁷P. de Silva and T. A. Wesolowski, *Phys. Rev. A* **85**, 032518 (2012).
- ³⁸A. M. P. Mendez, D. M. Mitnik, and J. E. Miraglia, *Int. J. Quantum Chem.* **116**,
1182 (2016).
- ³⁹A. M. P. Mendez, D. M. Mitnik, and J. E. Miraglia, *Adv. Quantum Chem.* **76**,
117 (2018).
- ⁴⁰R. C. Morrison and G. Liu, *J. Comput. Chem.* **13**, 1004 (1992).
- ⁴¹J. Cioslowski, P. Piskorz, and G. Liu, *J. Chem. Phys.* **107**, 6804 (1997).
- ⁴²U. Bozkaya, *J. Chem. Phys.* **139**, 154105 (2013).
- ⁴³U. Bozkaya, *J. Chem. Theory Comput.* **10**, 2041 (2014).
- ⁴⁴O. W. Day, Jr. and D. W. Smith, in *Reduced Density Operators with Applications
to Physical and Chemical Systems-II*, edited by R. M. Erdahl (Queen's University,
Kingston, ON, 1974), pp. 177–187.
- ⁴⁵O. W. Day, D. W. Smith, and C. Garrod, *Int. J. Quantum Chem. Symp.* **8**, 501
(1974).
- ⁴⁶D. W. Smith and O. W. Day, *J. Chem. Phys.* **62**, 113 (1975).
- ⁴⁷P. Politzer, J. S. Murray, and M. E. Grice, *Collect. Czech. Chem. Commun.* **70**,
550 (2005).
- ⁴⁸P. Politzer, Z. Peralta-Inga Shields, F. A. Bulat, and J. S. Murray, *J. Chem. Theory
Comput.* **7**, 377 (2011).
- ⁴⁹J. S. Murray, Z. Peralta-Inga Shields, P. Lane, L. Macaveiu, and F. A. Bulat, *J.
Mol. Model.* **19**, 2825 (2013).
- ⁵⁰J. J. Brown and S. L. Cockroft, *Chem. Sci.* **4**, 1772 (2013).
- ⁵¹W. M. Huo and E. N. Lassette, *J. Chem. Phys.* **72**, 2374 (1980).
- ⁵²C. L. Davis, H.-J. A. Jensen, and H. J. Monkhorst, *J. Chem. Phys.* **80**, 840
(1984).
- ⁵³C. L. Davis and H. J. Monkhorst, *J. Chem. Phys.* **81**, 5845 (1984).
- ⁵⁴P. E. Regier, J. Fisher, B. S. Sharma, and A. J. Thakkar, *Int. J. Quantum Chem.*
28, 429 (1985).
- ⁵⁵Q. Qu and E. A. Carter, *J. Chem. Theory Comput.* **14**, 5680 (2018).